

**Microwave emissivity
variability of
snow-covered sea ice**

S. Willmes et al.

The microwave emissivity variability of snow covered first-year sea ice from late winter to early summer: a model study

S. Willmes¹, M. Nicolaus², and C. Haas³

¹University of Trier, Environmental Meteorology, 54286 Trier, Germany

²Sea Ice Physics, Helmholtz-Zentrum für Polar- und Meeresforschung, 27570 Bremerhaven, Germany

³Earth and Space Science and Engineering, York University, Toronto, Canada

Received: 14 October 2013 – Accepted: 17 November 2013 – Published: 3 December 2013

Correspondence to: S. Willmes (willmes@uni-trier.de)

Published by Copernicus Publications on behalf of the European Geosciences Union.

Title Page

Abstract

Introduction

Conclusions

References

Tables

Figures

⏪

⏩

◀

▶

Back

Close

Full Screen / Esc

Printer-friendly Version

Interactive Discussion



Abstract

Satellite observations of microwave brightness temperatures between 19 GHz and 85 GHz are the main data source for operational sea-ice monitoring. However, the sea ice microwave emissivity is subject to pronounced seasonal variations and shows significant hemispheric contrasts that mainly arise from differences in the rate and strength of snow metamorphism and melt. We use the thermodynamic snow model SNTHERM and the microwave emission model MEMLS to identify the contribution of regional patterns in atmospheric energy fluxes to surface emissivity variations on Arctic and Antarctic sea ice between 2000 and 2009. The obtained emissivity data reveal a pronounced seasonal cycle with a large regional variability. The emissivity variability increases from winter to early summer and is more pronounced in the Antarctic. In the pre-melt period (January–May, July–November) the variations in surface microwave emissivity due to diurnal, regional and inter-annual variability of atmospheric forcing reach up to 3.4 %, 4.3 %, and 9.7 % for 19 GHz, 37 GHz and 85 GHz channels, respectively. Small but significant emissivity trends can be observed in the Weddell Sea during November and December as well as in Fram Strait during February. The obtained emissivity data lend themselves for an assessment of sea-ice concentration and snow-depth algorithm accuracies.

1 Introduction

The temporal and spatial variability of sea ice and its physical properties are operationally observed with satellite passive microwave radiometers since more than 30 yr (e.g. Eppler et al., 1992; Gloersen et al., 1992; Bjørgo et al., 1997). As one of the most important parameters in an operational global monitoring of the polar oceans sea-ice concentration is derived daily in the Arctic and Southern Oceans (e.g., Comiso et al., 1997; Comiso and Nishio, 2008; Cavalieri et al., 1996; Spreen et al., 2008). A retrieval of the fractional coverage of sea ice per pixel is based on the microwave emissivity con-

TCD

7, 5711–5734, 2013

Microwave emissivity variability of snow-covered sea ice

S. Willmes et al.

Title Page

Abstract

Introduction

Conclusions

References

Tables

Figures

◀

▶

◀

▶

Back

Close

Full Screen / Esc

Printer-friendly Version

Interactive Discussion



Microwave emissivity variability of snow-covered sea ice

S. Willmes et al.

Title Page

Abstract

Introduction

Conclusions

References

Tables

Figures

◀

▶

◀

▶

Back

Close

Full Screen / Esc

Printer-friendly Version

Interactive Discussion



trast of sea ice and the open ocean at microwave frequencies from 6 GHz to 90 GHz (e.g. Comiso, 1986; Gloersen et al., 1992; Cavalieri et al., 1997; Lubin et al., 1997; Svendsen et al., 1987). A more detailed retrieval of sea-ice and snow properties, e.g. thickness, roughness, age (e.g. Markus et al., 2006; Haas, 2001) from satellite microwave data is subject to regional, seasonal and hemispheric peculiarities and most often strictly dependent on the availability of coincident field measurements. Any retrieval technique for sea-ice characteristics based on passive microwave data relies on emissivity proxies that are derived from the microwave brightness temperature data at different channels and polarizations (e.g. Comiso et al., 1997, 2003; Spreen et al., 2008). From a comparison with field data or other ground-truth references tie points or transfer functions are deducted to allow for an inversion from microwave measurements to sea-ice concentration or surface properties like snow thickness (Markus and Cavalieri, 1998; Markus et al., 2006). Critical to this inversion are, however, seasonal and regional variations in the surface microwave emissivity that are caused by differences in atmospheric forcing and associated snow processes (Meier and Notz, 2010). As shown by Andersen et al. (2007) variations in sea-ice concentration retrievals over high-concentration Arctic sea ice are affected by anomalous snow emissivities. Their study concludes that long-term trends in surface and atmospheric properties influence computed trends in sea-ice extent and area through their undetermined impact on microwave emissivities.

As far as hemispheric contrasts are concerned the seasonal progression of snow decay differs significantly between the Arctic and the Antarctic (Andreas and Ackley, 1982; Nicolaus et al., 2006). The stage of advanced melt (Livingstone et al., 1997) that is characterized by persistent snowmelt during summer is dominant in the Arctic (Comiso and Kwok, 1996; Garrity, 1992) while diurnal freeze-thaw cycles prevail on Antarctic sea ice (Willmes et al., 2006, 2009). The microwave emissivity of snow-covered sea ice is not only sensitive to the presence of meltwater but varies with uncertain strength along with the seasonal changes that occur in snow stratification, grain sizes, layering and density already during the pre-melt period. For instance the problem that layered

snow causes a low sea-ice concentration bias has been identified and described by e.g. Cavalieri et al. (1990), Comiso et al. (1997) and effects of snow layering during late summer on sea-ice concentration retrieval were evaluated by Markus and Dokken (2002).

5 In this paper we investigate the variability of the microwave emissivity of snow-covered first-year ice (FYI) from a combined thermodynamic/microwave model approach. We examine the processes involved with atmospherically driven snow metamorphism and their effect on the microwave properties of snow-covered sea ice in the Arctic and Antarctic. We do not take into account a pre-conditioning of the snow cover,
10 nor do we try to simulate snow accumulation, flooding and the effect of basal heat fluxes. Our approach is based on an idealized initial snow cover that is exposed to typical atmospheric forcing in either hemisphere. We want to identify the contribution of regional patterns in atmospheric energy fluxes to surface emissivity variations on Arctic and Antarctic sea ice and the resulting hemispheric contrasts in the seasonal
15 microwave brightness temperature (T_b) evolution. We use the one-dimensional snow model SNTHERM (Jordan, 1991; Nicolaus et al., 2006) and the Microwave Emission Model for Layered Snowpacks (MEMLS, Wiesmann and Mätzler, 1999), adapted to snow on sea ice by Tonboe et al. (2006). With the results presented here we want to provide a dataset of the seasonal variability and regional specifications of the microwave
20 emissivity variability of FYI in the 19 to 85 GHz frequency range. This dataset lends itself for an assessment and improvement of potential accuracies of sea-ice and snow retrieval algorithms that are based on any form of emissivity patterns.

2 Data and methods

25 Physical snow properties of a layered snow pack on sea ice are simulated by the one-dimensional energy- and mass-balance model SNTHERM. The model was created by Jordan (1991) and adapted and applied to sea ice by Jordan et al. (1999) and Andreas et al. (2004). Here we use the latest version by Nicolaus et al. (2006) and we perform

Microwave emissivity variability of snow-covered sea ice

S. Willmes et al.

Title Page

Abstract

Introduction

Conclusions

References

Tables

Figures

◀

▶

◀

▶

Back

Close

Full Screen / Esc

Printer-friendly Version

Interactive Discussion



**Microwave emissivity
variability of
snow-covered sea ice**

S. Willmes et al.

Title Page

Abstract

Introduction

Conclusions

References

Tables

Figures

◀

▶

◀

▶

Back

Close

Full Screen / Esc

Printer-friendly Version

Interactive Discussion



similar experiments, starting each simulation with a new initialization in winter (Arctic: January, Antarctic: July). We chose SNTHERM since it allows for high-resolution (mm-scale) simulations of the seasonal evolution of a snow pack on sea ice as a function of atmospheric forcing and initial stratigraphy. Representing all snow layers by distinct control volumes in a moving vertical grid has the advantage of treating natural stratigraphic units within the snow. SNTHERM was forced with six-hourly data of the 2 m air temperature, relative humidity, 10 m wind speed, incoming shortwave radiation and downward longwave radiation from the European Center for Medium Range Weather Forecast (ECMWF) ERA interim data at 0.75° resolution (Dee et al., 2011).

The Microwave Emission Model for Layered Snowpacks (MEMLS, Wiesmann and Mätzler, 1999; Mätzler and Wiesmann, 1999) is used to compute microwave brightness temperatures from vertical snow profiles. We use a sea ice version of MEMLS (Tonboe et al., 2006; Tonboe, 2010) to account for the effect of sea-ice dielectric properties on microwave brightness temperatures. The model calculates T_b at frequencies between 5 GHz and 200 GHz for vertical and horizontal polarizations. Here we use T_b values at frequencies of 19 GHz, 37 GHz and 85 GHz (hereafter referred to as 19V, 19H, 37V, 37H, 85H and 85V), to compare results with the sensors used in operational satellite microwave monitoring, i.e. the Special Sensor Microwave Imager (SSM/I) radiometer and (with similar frequencies) the Advanced Microwave Scanning Radiometer (AMSR). All simulations are at 50° incidence angle, as typical for conically scanning radiometers.

SNTHERM and MEMLS are used in a combined model study to infer the temporal evolution of sea-ice microwave brightness temperatures for typical atmospheric forcing conditions in the Arctic and Antarctic. Since we focus on the surface forcing, we neglect the basal (ocean) heat flux and sea-ice growth. Instead, we perform our experiments with 60 cm of sea ice with a density of 910 kg m^{-3} that is covered with an initial snow profile with 30 cm thickness. The snow layer at initialization is represented by 30 layers of 1 cm thickness with a density of 320 kg m^{-3} and a snow grain size of 1 mm. Below the snow we add 12 layers of sea ice with 5 cm thickness and a salinity of 7 ppt.

Microwave emissivity variability of snow-covered sea ice

S. Willmes et al.

Title Page

Abstract

Introduction

Conclusions

References

Tables

Figures

◀

▶

◀

▶

Back

Close

Full Screen / Esc

Printer-friendly Version

Interactive Discussion



Although regional differences in snow depth and snow stratigraphies are documented (e.g. Warren et al., 1999; Massom et al., 2001; Nicolaus et al., 2009) we set this model experiment up with the same initialization profile in all considered regions. This approach enables us to identify the net effect of atmospheric forcing on regional changes in the microwave emissivity, without strong impacts of the initial (winter) snow properties. Our simulations are not able to reproduce flooding and snow-ice formation, snowfall is also not considered. With this setup, however, we are able to identify the isolated contribution of regional patterns in atmospheric energy fluxes to surface emissivity variations.

The temperature in the lowest ice layer is assumed to be at the freezing point of -1.8°C while the initial snow surface temperature is set to the ERA interim air temperature for each position and year. Linear temperature profiles are assumed in sea ice and snow with the temperature at the snow/ice interface representing one third of the total temperature gradient from the sea-ice bottom to the snow surface.

We created forcing data for SNTHERM from six-hourly ERA interim reanalysis for 10 yr (2000 to 2009), at 34 positions for 8 different regions in the Arctic (January to June) and at 29 positions for 6 regions in the Antarctic (July to December, Fig. 1) where sea ice is regularly present at the start of simulations and remains on average at least until May (Arctic) or November (Antarctic).

The interface between the snow and the emission model is provided by the vertical profiles of snow temperature, density, grain size and wetness. The optical grain diameter d_o provided by SNTHERM was recalculated into the exponential correlation length ρ_{ex} for usage in MEMLS according to Eq. (1), where ρ_s and ρ_i are snow and ice densities in kg m^{-3} , respectively (Mätzler, 2002).

$$\rho_{\text{ex}} = F \cdot d_o \cdot (1 - \rho_s \cdot \rho_i^{-1}) \quad (1)$$

The scaling coefficient F in Eq. (1) is adjusted to ensure the best alignment of our simulated Tb data with the NasaTeam FYI tie points (Cavaliere et al., 1994) after 5 days of SNTHERM spin-up time. In doing so, a value of 0.12 was obtained for F . The use

of a correlation length correction scheme for microwave modeling has recently been demonstrated by Langlois et al. (2012).

In many algorithms, microwave brightness temperatures are used in form of either a polarization ratio (PR, Eq. 1) or a gradient ratio (GR, Eq. 2) using different microwave polarizations and frequencies.

$$PR = (19V - 19H) \cdot (19V + 19H)^{-1} \quad (2)$$

$$GR = (37V - 19V) \cdot (37V + 19V)^{-1} \quad (3)$$

With these two parameters the observation of emissivity variations is enabled by eliminating the contribution of the effective temperature variability. Here, we use PR and GR, together with the microwave emissivities at different polarizations and frequencies to investigate their seasonal changes in context with the prevailing atmospheric forcing in different regions.

For a comparison with satellite data we use the DMSP SSM/I-SSMIS Daily Polar Gridded Brightness Temperatures dataset (Maslanik and Stroeve, 2004) provided by the US National Snow and Ice Data Center (NSIDC). Sea Ice Concentrations from Nimbus-7 SMMR and DMSP SSM/I-SSMIS Passive Microwave Data product (Cavalieri et al., 1996) were used to create a subset of satellite microwave brightness temperatures at high sea-ice concentrations only.

3 Results

The simulated brightness temperatures are shown in feature spaces of PR/GR (Fig. 2a and b) and of 37V/19V (Fig. 2c and d) for the Arctic and Antarctic, respectively. Data extracted from daily polar gridded satellite Tb (Maslanik and Stroeve, 2004) are shown by grey areas for all regions where the sea-ice concentration exceeds 90 %. The lines of 100 % sea-ice concentrations for the NasaTeam (Cavalieri et al., 1984, 1994) and Bootstrap algorithms (Comiso, 1986) are shown by white dotted lines. The

Microwave emissivity variability of snow-covered sea ice

S. Willmes et al.

Title Page

Abstract

Introduction

Conclusions

References

Tables

Figures

◀

▶

◀

▶

Back

Close

Full Screen / Esc

Printer-friendly Version

Interactive Discussion



5 simulated data align well close to the 100% sea-ice concentration lines revealing at the same time a distinct variability that is more pronounced in the Antarctic within both feature spaces. Especially during the last month of our simulation period (Arctic: June, Antarctic: December), the beginning effect of surface melt causes the position of the
10 simulated snow profile to move towards the open water tie point. This is expressed by elongated clusters pointing towards lower sea-ice concentrations mainly for the Arctic simulations.

The microwave emissivities at 19, 37 and 85 GHz are characterized by a pronounced seasonal variability within the simulated period (Fig. 3). The seasonal cycle for all presented frequencies and both polarizations is stronger in the Arctic with a substantial increase occurring in the month of June (Fig. 3a and c). This emissivity increase is attributed to the onset of the advanced melt stage (Livingstone et al., 1997; Drobot and Anderson, 2001; Markus et al., 2009; Belchansky et al., 2004), when the presence of meltwater within the snow becomes persistent throughout the day. In the Antarctic (Fig. 3b and d) the regional differences in emissivities are more distinct than in the Arctic. The advanced melt stage is found with much lower probability than in the Arctic (Willmes et al., 2006, 2009). The observed tendency towards higher emissivities in the Antarctic at the beginning of summer is rather an effect of averaging single profiles where temporally limited thaw events causing very high emissivities for the duration of
20 melt are occurring at different points in time. The different melt process in the two hemispheres are described by a study of Nicolaus et al. (2006). They show that the impact of melting and evaporation the snow cover decrease is very different between Arctic and Antarctic, e.g. the ratio of evaporated snow mass to melted snow mass per unit area amounts to approximately 4.2 in the Antarctic and only 0.75 in the Arctic, which
25 certainly also impacts the evolution of microwave emissivities.

The probability distribution of emissivities vs. region is given in Fig. 4 for different polarizations and frequencies, exemplary for the 4th month of simulations (Arctic: April, Antarctic: October). As denoted by the mean (squares) and standard deviations (crosses) the observed regions show pronounced differences in their emissivity vari-

Microwave emissivity variability of snow-covered sea ice

S. Willmes et al.

[Title Page](#)[Abstract](#)[Introduction](#)[Conclusions](#)[References](#)[Tables](#)[Figures](#)[Back](#)[Close](#)[Full Screen / Esc](#)[Printer-friendly Version](#)[Interactive Discussion](#)

riod than 19 GHz, which is an effect of their limited penetration depth and the resulting larger impact of changes in the snow cover.

The average seasonal evolution of the microwave emissivity as well as of PR and GR in both hemispheres is subsumed in Fig. 5. The diurnal and regional emissivity variability increases from late winter to early summer for all frequencies in both hemispheres while it is in general larger in the Antarctic throughout the season (Fig. 5a, crosses). The Arctic experiences the largest increase in emissivity variability from the months of May to June, when persistent melt initiates in some regions. The hemispheric contrast increases with frequency. Similar observations hold for the monthly values of PR and GR (Fig. 5b). Especially the GR variability during the pre-melt period is more pronounced in the Antarctic. In comparison to Fig. 4 the presented values point out that the regional emissivity variability can deviate substantially from the average hemispheric variability. For example, the standard deviation of 37 V during October is 0.038 in the BA region and 0.018 in the WP region (compare Fig. 4b), while it is 0.029 when the entire Antarctic is considered. This finding is critical for the formulation of tie points that are valid for an entire hemisphere and suggests to take regional specifications into account.

Some snow characteristics pointing towards an explanation of hemispheric differences in seasonal emissivity variability are indicated in Fig. 6. The mean monthly microwave snow penetration depth is significantly lower in the Arctic during month 6 (5 and 6) for 19 V (37 V). Penetration into the ice is here considered 30 cm (equals maximum snow thickness) penetration and hence no higher values are obtained. The rate of decrease in penetration depth is smaller for 19 V. This points out the stronger sensitivity of T_b values at 37 GHz to atmospheric variability and associated changes in the vertical snow profile. In the pre-melt period, the bulk snow density increases on average faster in the Antarctic (Fig. 6b). This is rapidly reversed when the advanced melt starts in the Arctic in June and wet snow with high densities is prevalent. Monthly hemispheric average 37 V emissivities are higher in the Antarctic (Fig. 6c) and less sensitive to a decrease in penetration depth before the melt season starts. This reveals

Microwave emissivity variability of snow-covered sea ice

S. Willmes et al.

Title Page

Abstract

Introduction

Conclusions

References

Tables

Figures

◀

▶

◀

▶

Back

Close

Full Screen / Esc

Printer-friendly Version

Interactive Discussion



that the processes that cause the penetration depth to cease throughout the season have a larger impact on the mean 37 V emissivity in the Arctic than in the Antarctic. As shown above, however, this does not hold for the emissivity variability, which is larger in the Antarctic.

Trends in emissivity were derived for both hemispheres and for all regions separately. Our data revealed that significant trends ($\alpha = 0.05$) are found almost exclusively in the Weddell Sea (WS) region for all channels (except 19 H) in the months of November and December. Although being very small (0.01, 0.04 and 0.08 per decade in the month of December for 19 V, 37 V and 85 V, respectively) the 10 yr time series gives indication for a tendency towards larger emissivities that might be associated with increased melt rates or earlier melt onset. Apart from the WS, very small but significant trends are only found for the FS region in February (19 V: $0.005 \text{ decade}^{-1}$, 37 V: $0.007 \text{ decade}^{-1}$) and for BF in June (85H: 0.04 decade^{-1}).

4 Discussion and conclusions

It is well known that the accuracy of sea-ice concentration algorithms is estimated to be on average not better than $\pm 5\%$ (Meier and Notz, 2010; Meier, 2005). With the data presented here, algorithm accuracies for high-concentration sea ice can be determined with regional and seasonal reference. Sources of ambiguity for sea-ice concentration and snow depth retrieval are manifold and variations in emissivity just represent one problem next to spatial inhomogeneity of surfaces, the presence of thin ice (Kwok et al., 1997) and atmospheric disturbances (e.g. Cavalieri et al., 1995; Markus and Dokken, 2002; Spreen et al., 2008). We consider the presented emissivity variability representative for the atmospherically induced variability found over high-concentration sea ice. Even if an algorithm implements monthly tie points to account for seasonal variations and weather effects (Markus and Cavalieri, 2000; Gloersen and Cavalieri, 1986), this tie point refers to an emissivity value that will miss the regional, diurnal and inter-annual emissivity variations inherent to a specific region.

Microwave emissivity variability of snow-covered sea ice

S. Willmes et al.

Title Page

Abstract

Introduction

Conclusions

References

Tables

Figures

◀

▶

◀

▶

Back

Close

Full Screen / Esc

Printer-friendly Version

Interactive Discussion



**Microwave emissivity
variability of
snow-covered sea ice**

S. Willmes et al.

Title Page

Abstract

Introduction

Conclusions

References

Tables

Figures

◀

▶

◀

▶

Back

Close

Full Screen / Esc

Printer-friendly Version

Interactive Discussion



Atmospheric effects could probably smooth the emissivity variability we present here. Nevertheless we consider our results as a seasonal background variability that needs to be taken into account even when weather filters are applied. An assessment of the contribution of different sources for varying brightness temperatures over high-concentration sea ice goes however beyond the scope of this paper. We did not include the effect of flooding and snow ice formation and hence, the contribution of salty slush and gap layers that probably play an important role for microwave brightness temperatures found over Antarctic sea ice as well (Massom et al., 2001; Haas et al., 2001; Nicolaus et al., 2009). We suggest the spatio-temporal emissivity impact of these processes to be quantified separately such that an assessment of combined ambiguities and their regional characteristics is enabled.

A monthly and regionally determined microwave emissivity variability as presented in this study can help in determining optimized tie points for the definition of transfer functions from raw brightness temperature measurements to sea-ice surface properties. In addition, the potential for an improved snow depth retrieval can be investigated from the combined snow and microwave data.

The thermodynamic snow model SNTHERM and the microwave emission model for layered snowpacks (MEMLS) were used to identify the contribution of regional patterns in atmospheric energy fluxes to surface emissivity variations on Arctic and Antarctic sea ice between 2000 and 2009.

The microwave emissivities at 19, 37 and 85 GHz are characterized by a pronounced seasonal variability within the simulated period. The combined regional, diurnal and inter-annual emissivity variability increases from winter to early summer and Antarctic regions are affected by a larger range of emissivity values with a tendency towards higher mean emissivities than in the Arctic. In the pre-melt period, the variations in surface microwave emissivity due to diurnal, regional and inter-annual variability of atmospheric forcing reach up to 2.6 %, 3.7 %, and 7.8 % for 19 GHz, 37 GHz and 85 GHz channels, respectively.

Significant emissivity trends are found in the Weddell Sea (WS) region for all channels (except 19H) in November and December, which might be associated with increased melt rates or earlier melt onset.

The obtained emissivity data characterize the background emissivity variability of snow-covered first-year sea ice due to atmospheric forcing and lend themselves for an assessment and improvement of sea-ice concentration and snow-depth algorithm accuracies.

Acknowledgements. This work was supported by the Deutsche Forschungsgemeinschaft (DFG) in the framework of the priority programme “Antarctic Research with comparative investigations in Arctic ice areas” by a grant to WI 33114/-1 and WI 3314/-2. We are very grateful to Rasmus T. Tonboe from the Danish Meteorological Institute who kindly provided his sea ice version of MEMLS. Sea-ice brightness temperatures and sea ice concentrations were provided by the US National Snow and Ice Data Center (NSIDC). The European Center for Medium Range Weather Forecast (ECMWF) offered ERA interim data free of charge. Leif Toudal Pedersen, Rasmus Tonboe and Günther Heinemann provided very valuable comments on this research.

References

- Andersen, S., Tonboe, R., Kaleschke, L., Heygster, G., and Pedersen, L. T.: Intercomparison of passive microwave sea ice concentration retrievals over the high-concentration Arctic sea ice, *J. Geophys. Res.*, 112, C08004, doi:10.1029/2006JC003543, 2007.
- Andreas, E. L. and Ackley, S. F.: On the differences in ablation seasons of Arctic and Antarctic sea ice, *J. Atmos. Sci.*, 389, 440–447, 1982.
- Andreas, E. L., Jordan, R. E., and Makshtas, A. P.: Simulations of snow, ice and near-surface atmospheric processes on ice station Weddell, *J. Hydrometeorol.*, 5, 611–624, 2004.
- Belchansky, G., Douglas, D. C., Mordvintsev, I., and Platonov, N.: Estimating the time of melt onset and freeze onset over Arctic sea ice area using active and passive microwave data, *Remote Sens. Environ.*, 92, 21–39, 2004.
- Bjørge, E., Johannessen, O. M., and Miles, M. W.: Analysis of merged SMMR-SSM/I time series of Arctic and Antarctic sea ice parameters 1978–1995, *Geophys. Res. Lett.*, 24, 413–416, 1997.

Microwave emissivity variability of snow-covered sea ice

S. Willmes et al.

Title Page

Abstract

Introduction

Conclusions

References

Tables

Figures



Back

Close

Full Screen / Esc

Printer-friendly Version

Interactive Discussion



Microwave emissivity variability of snow-covered sea ice

S. Willmes et al.

Title Page

Abstract

Introduction

Conclusions

References

Tables

Figures

◀

▶

◀

▶

Back

Close

Full Screen / Esc

Printer-friendly Version

Interactive Discussion



- Cavaliere, D. J.: A microwave technique for mapping thin ice, *J. Geophys. Res.*, 99, 12561–12572, 1994.
- Cavaliere, D. J., Gloersen, P., and Campbell, W. J.: Determination of sea-ice parameters with the NIMBUS 7 scanning multichannel microwave radiometer, *J. Geophys. Res.*, 89, 5355–5369, 1984.
- 5 Cavaliere, D. J., Burns, B. A., and Onstott, R. G.: Investigation of the effects of summer melt on the calculation of sea ice concentration using active and passive microwave data, *J. Geophys. Res.*, 95, 5359–5369, 1990.
- Cavaliere, D. J., St. Germain, K. M., and Swift, C. T.: Reduction of weather effects in the calculation of sea-ice concentration with the DMSP SSM/I, *J. Glaciol.*, 41, 455–464, 1995.
- 10 Cavaliere, D. J., Parkinson, C. L., Gloersen, P., and Zwally, H. J.: Sea Ice Concentrations from Nimbus-7 SMMR and DMSP SSM/I-SSMIS Passive Microwave Data, [2002–2009], National Snow and Ice Data Center, Boulder, Colorado USA, Digital media, updated yearly, 1996.
- Cavaliere, D. J., Parkinson, C. L., Gloersen, P., and Zwally, H. J.: Arctic and Antarctic Sea Ice Concentrations from Multichannel Passive-microwave Satellite Data Sets: October 1978 to December 1996, User's Guide, NASA Technical Memorandum 104647, 17 pp., 1997.
- 15 Comiso, J. C.: Characteristics of Arctic winter sea ice from satellite multispectral microwave observations, *J. Geophys. Res.*, 91, 975–994, 1986.
- Comiso, J. C. and Kwok, R.: Surface and radiative characteristics of the summer Arctic sea ice cover from multisensory satellite observations, *J. Geophys. Res.*, 101, 28397–28416, 1996.
- 20 Comiso, J. C. and Nishio, F.: Trends in the sea ice cover using enhanced and compatible AMSR-E, SSM/I, and SMMR data, *J. Geophys. Res.*, 113, C02S07, doi:10.1029/2007JC004257, 2008.
- Comiso, J. C., Cavaliere, D. J., Parkinson, C. L., and Gloersen, P.: Passive microwave algorithms for sea ice concentration: a comparison of two techniques, *Remote Sens. Environ.*, 60, 357–384, 1997.
- 25 Comiso, J. C., Cavaliere, D. J., and Markus, T.: Sea ice concentration, ice temperature, and snow depth using AMSR-E data, *IEEE T. Geosci. Remote*, 41, 243–252, doi:10.1109/TGRS.2002.808317, 2003.
- 30 Dee, D. P. and 35 others: The ERA-Interim reanalysis: configuration and performance of the data assimilation system, *Q. J. Roy. Meteor. Soc.*, 137, 553–597, doi:10.1002/qj.828, 2011.

Microwave emissivity variability of snow-covered sea ice

S. Willmes et al.

Title Page

Abstract

Introduction

Conclusions

References

Tables

Figures

◀

▶

◀

▶

Back

Close

Full Screen / Esc

Printer-friendly Version

Interactive Discussion



Drobot, S. D. and Anderson, M. R.: An improved method for determining snowmelt onset dates over Arctic sea ice using SMMR and SSM/I data, *J. Geophys. Res.*, 106, 24033–24049, 2001.

5 Eppler, D., Farmer, L., Lohanick, A., Anderson, M., Cavalieri, D., Comiso, J., Gloersen, P., Garity, C., Grenfell, T., Hallikainen, M., Maslanik, J., Mätzler, C., Melloh, R., Rubinstein, I., and Swift, C.: Passive microwave signatures of sea ice, in: *Microwave Remote Sensing of Sea Ice*, edited by: Carsey, F. D., no. 68 in *Geophysical Monograph*, American Geophysical Union, 1992.

10 Garrity, C.: Characterization of snow on floating ice and case studies of brightness temperature changes during the onset of melt, in: *Microwave Remote Sensing of Sea Ice*, edited by: Carsey, F. D., no. 68 in *Geophysical Monograph*, American Geophysical Union, 1992.

Gloersen, P. and Cavalieri, D. J.: Reduction of weather effects in the calculation of sea ice concentration from microwave radiances, *J. Geophys. Res.*, 91, 3913–3919, 1986.

15 Gloersen, P., Campbell, W. J., Cavalieri, D. J., Comiso, J. C., Parkinson, C. L., and Zwally, H. J.: Arctic and Antarctic Sea Ice, 1978–1987: Satellite passive-microwave observations and analysis, *NASA Special Publications*, 511, 290 pp., 1992.

Haas, C.: The seasonal cycle of ERS scatterometer signatures over perennial Antarctic sea ice and associated surface ice properties and processes, *Ann. Glaciol.*, 33, 69–73, 2001.

20 Haas, C., Thomas, D. N., and Bareiss, J.: Surface properties and processes of perennial Antarctic sea ice in summer, *J. Glaciol.*, 47, 613–625, 2001.

Jordan, R. E.: A one-dimensional temperature model for a snow cover, *Special Report 91–16*, US Army Corps of Eng. Cold Regions Research and Engineering Laboratory, Hanover, NH, 1991.

25 Jordan, R. E., Andreas, E. L., and Makshtas, A. P.: Heat budget of snow-covered sea ice at North Pole 4, *J. Geophys. Res.*, 104, 7785–7806, 1999.

Kwok, R., Comiso, J. C., Martin, S., and Drucker, R.: Ross Sea polynyas: response of ice concentration retrievals to large areas of thin ice, *J. Geophys. Res.*, 112, C12012, doi:10.1029/2006JC003967, 2007.

30 Langlois, A., Royer, A., Derksen, C., Montpetit, B., Dupont, F., and Gota, K.: Coupling the snow thermodynamic model SNOWPACK with the microwave emission model of layered snowpacks for subarctic and Arctic snow water equivalent retrievals, *Water Resour. Res.*, 48, W12524, doi:10.1029/2012WR012133, 2012.

Microwave emissivity variability of snow-covered sea ice

S. Willmes et al.

Title Page

Abstract

Introduction

Conclusions

References

Tables

Figures

◀

▶

◀

▶

Back

Close

Full Screen / Esc

Printer-friendly Version

Interactive Discussion



- Livingstone, C. E., Onstott, R. G., Arsenault, L. D., Gray, A. L., and Singh, K. P.: Microwave sea-ice signatures near the onset of melt, *IEEE T. Geosci. Rem.*, 25, 174–187, 1997.
- Lubin, D., Garrity, C., Ramseier, R. O., and Whritner, R. H.: Total sea ice concentration retrieval from the SSM/I 85.5 GHz channels during the Arctic summer, *Remote Sens. Environ.*, 62, 63–76, 1997.
- 5 Mätzler, C.: Relation between grain-size and correlation length of snow, *J. Glaciol.*, 48, 461–466, 2002.
- Mätzler, C. and Wiesmann, A.: Extension of the microwave emission model of layered snow-packs to coarse-grained snow, *Remote Sens. Environ.*, 70, 317–325, 1999
- 10 Markus, T. and Cavalieri, D. J.: Snow depth distribution over sea ice in the Southern Ocean from satellite passive microwave data, *Antarctic sea ice: physical processes, interactions, and variability*, *Antarct. Res. Ser.*, 74, 19–39, 1998.
- Markus, T. and Cavalieri, D. J.: An enhancement of the NASA Team sea ice algorithm, *IEEE T. Geosci. Rem.*, 38, 1387–1398, 2002.
- 15 Markus, T. and Dokken, S.: Evaluation of late summer passive microwave Arctic sea ice retrievals, *IEEE T. Geosci. Rem.*, 40, 348–356, 2000.
- Markus, T., Powell, D. C., and Wang, J. R.: Sensitivity of passive microwave snow depth retrievals to weather effects and snow evolution, *IEEE T. Geosci. Rem.*, 44, 68–77, 2006.
- Markus, T., Stroeve, J. C., and Miller, J.: Recent changes in Arctic sea ice melt onset, freezeup, and melt season length, *J. Geophys. Res.*, 114, C12024, doi:10.1029/2009JC005436, 2009.
- 20 Maslanik, J. and Stroeve, J. C.: DMSP SSM/I-SSMIS Daily Polar Gridded Brightness Temperatures, Version 4, 2000–2009, NASA DAAC at the National Snow and Ice Data Center, Boulder, Colorado, USA, 2004, updated 2012.
- Massom, R. A., Eicken, H., Haas, C., Jeffris, M. O., Drinkwater, M. R., Sturm, M., Worby, A. P., Wu, X., Lytle, V. I., Ushio, S., Morris, K., Reid, P. A., Warren, S. G., and Allison, I.: Snow on Antarctic ice, *Rev. Geophys.*, 39, 413–445, 2001.
- 25 Meier, W. and Notz, D.: A note on the accuracy and reliability of satellite-derived passive microwave estimates of sea-ice extent, *Climate and Cryosphere Sea Ice Working Group Consensus Document*, World Climate Research Program, 2010.
- 30 Meier, W. N.: Comparison of passive microwave ice concentration algorithm retrievals with AVHRR imagery in Arctic peripheral seas, *IEEE T. Geosci. Rem.*, 43, 1324–1337, 2005.

**Microwave emissivity
variability of
snow-covered sea ice**

S. Willmes et al.

Title Page

Abstract

Introduction

Conclusions

References

Tables

Figures

◀

▶

◀

▶

Back

Close

Full Screen / Esc

Printer-friendly Version

Interactive Discussion



Nicolaus, M., Haas, C., Bareiss, J., and Willmes, S.: A model study of differences of snow thinning on Arctic and Antarctic first-year sea ice during spring and summer, *Ann. Glaciol.*, 44, 147–153, 2006.

5 Nicolaus, M., Haas, C., and Willmes, S.: Evolution of first-year and second-year snow properties on sea ice in the Weddell Sea during spring-summer transition, *J. Geophys. Res.*, 114, D17109, doi:10.1029/2008JD011227, 2009.

Spreen, G., Kaleschke, L., and Heygster, G.: Sea ice remote sensing using AMSR-E 89 GHz channels, *J. Geophys. Res.*, 113, C02S03, doi:10.1029/2005JC003384, 2008.

10 Svendsen, E., Mätzler, C., and Grenfell, T. C.: A model for retrieving total sea ice concentration from a spaceborne dual-polarized passive microwave instrument operating near 90 GHz, *Int. J. Rem. Sens.*, 8, 1479–1487, 1987.

Tonboe, R. T.: The simulated sea ice thermal microwave emission at window and sounding frequencies, *Tellus A*, 62, 333–344, 2010.

15 Tonboe, R. T., Heygster, G., Pedersen, L. T., and Andersen, S.: Sea ice emission modelling, in: *Thermal Microwave Radiation: Applications for Remote Sensing*, edited by: Mätzler, C., IET Electromagnetic Wave Series, 52, London, UK, 382–400, 2006.

Warren, S. G., Rigor, I. G., Untersteiner, N., Radionov, V. F., Bryazgin, N. N., Aleksandrov, V., and Colony, R.: Snow depth on Arctic sea ice, *J. Climate*, 12, 1814–1829, 1999.

20 Wiesmann, A. and Mätzler, C.: Microwave emission model of layered snowpacks, *Remote Sens. Environ.*, 70, 307–316, 1999.

Willmes, S., Bareiss, J., Haas, C., and Nicolaus, M.: The importance of diurnal processes for the seasonal cycle of sea-ice microwave brightness temperatures during early summer in the Weddell Sea, Antarctica, *Ann. Glaciol.*, 44, 297–302, 2006.

25 Willmes, S., Haas, C., Bareiss, J., and Nicolaus, M.: Satellite microwave observations of the interannual variability of snowmelt on sea ice in the Southern Ocean, *J. Geophys. Res.*, 114, C03006, doi:10.1029/2008JC004919, 2009.

Microwave emissivity variability of snow-covered sea ice

S. Willmes et al.

Table 1. Mean and standard deviation of emissivities at 19, 37 and 85 GHz (vertical polarization) for different SN THERM initialization and MEMLS parameterization for region WS during October, derived from 4-times daily values, 2000–2009. REF: initialization profile used within this study, zs15: 15 cm snow depth, zs50: 50 cm snow depth, dg15: 1.5 mm grain size, S02: sea-ice salinity 2 ppt, S12: sea-ice salinity 12 ppt, D270: snow density 270 kg m⁻³, D370: snow density 370 kg m⁻³, lay1: an ice layer with 910 kg m⁻³ density is included in the middle of the profile right from the start.

		REF	zs15	zs50	dg15	S02	S12	D270	D370	lay1
e19v	mean	0.946	0.942	0.915	0.928	0.948	0.931	0.912	0.942	0.914
	std	0.01	0.01	0.02	0.01	0.01	0.01	0.02	0.01	0.02
e37v	mean	0.873	0.857	0.791	0.814	0.857	0.852	0.765	0.861	0.810
	std	0.03	0.05	0.05	0.05	0.03	0.03	0.06	0.04	0.05
e85v	mean	0.738	0.660	0.658	0.660	0.716	0.716	0.582	0.737	0.665
	std	0.07	0.10	0.08	0.08	0.06	0.06	0.09	0.07	0.09
PR	mean	0.048	0.048	0.042	0.046	0.041	0.053	0.043	0.048	0.074
	std	0.01	0.01	0.01	0.01	0.01	0.01	0.01	0.01	0.01
GR	mean	-0.040	-0.048	-0.073	-0.065	-0.050	-0.044	-0.088	-0.045	-0.060
	std	0.01	0.02	0.02	0.02	0.01	0.02	0.03	0.02	0.02

[Title Page](#)
[Abstract](#)
[Introduction](#)
[Conclusions](#)
[References](#)
[Tables](#)
[Figures](#)
[Back](#)
[Close](#)
[Full Screen / Esc](#)
[Printer-friendly Version](#)
[Interactive Discussion](#)


Microwave emissivity variability of snow-covered sea ice

S. Willmes et al.

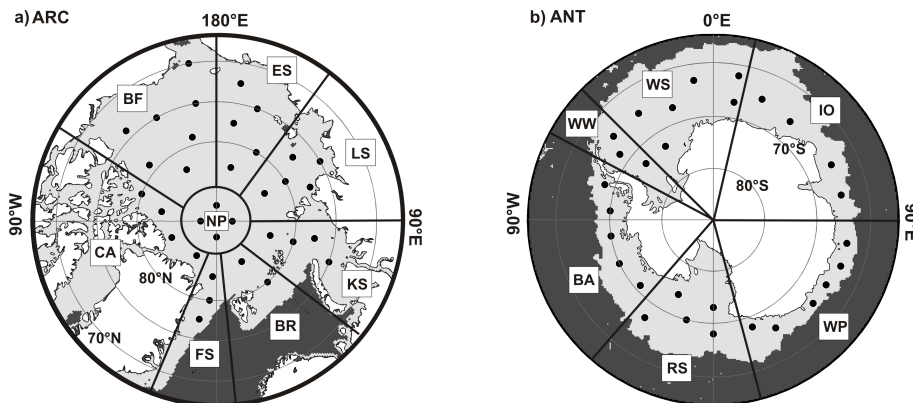


Fig. 1. Maps of the Arctic (**a**) and Antarctic (**b**) showing the location of the regions referred to and the positions where atmospheric forcing data were extracted. The grey area indicates the average sea-ice extent for 1 June (Arctic) and 1 December (Antarctic), 2000–2009. Regions indicated are: Arctic: NP (North Pole), FS (Fram Strait), BR (Barents Sea), KS (Kara Sea), LS (Laptev Sea), ES (East Siberian Sea), BF (Beaufort Sea), CA (Canadian Arctic), Antarctic: WW (Western Weddell Sea), WS (Weddell Sea), IO (Indian Ocean), WP (Western Pacific), RS (Ross Sea), BA (Bellingshausen-Amundsen Sea).

[Title Page](#)
[Abstract](#)
[Introduction](#)
[Conclusions](#)
[References](#)
[Tables](#)
[Figures](#)
[◀](#)
[▶](#)
[◀](#)
[▶](#)
[Back](#)
[Close](#)
[Full Screen / Esc](#)
[Printer-friendly Version](#)
[Interactive Discussion](#)


Microwave emissivity variability of snow-covered sea ice

S. Willmes et al.

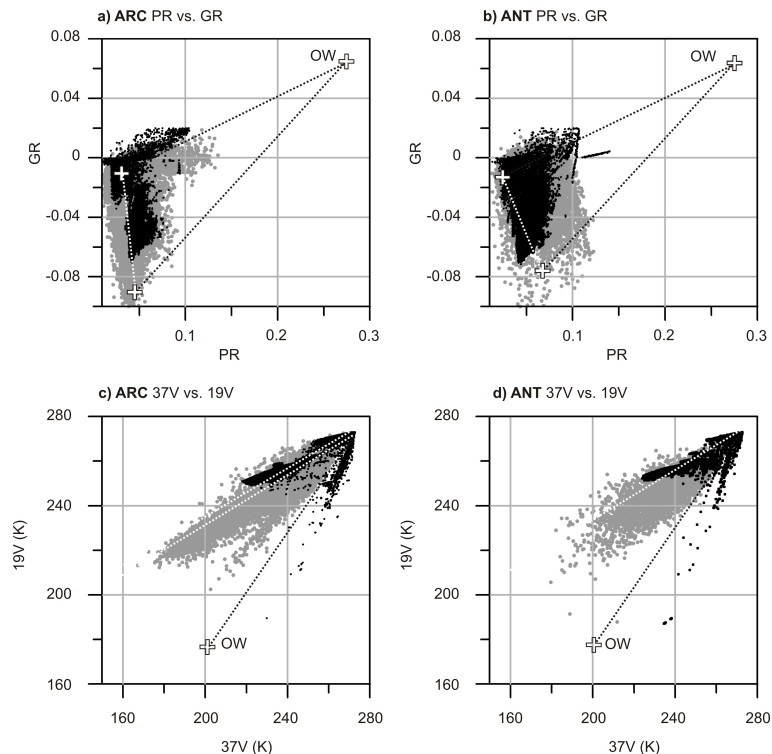


Fig. 2. Simulated brightness temperatures (black) in PR/GR feature space for the Arctic (**a**, January to June) and Antarctic (**b**, July to December) and in 37 V/19 V feature space for the Arctic (**c**) and Antarctic (**d**), 4 times daily data, 2000–2009. Daily values of observed satellite Tb for area with sea-ice concentrations above 90 % are shown by grey dots for comparison. Tie points for open water (OW) and (a, b only) first-year ice (FYI) as well as multi-year ice (MYI) are indicated by crosses. 100 % sea ice concentration lines are shown by white dotted lines, while different lines in (**c**) show lines for summer and winter, respectively.

Microwave emissivity variability of snow-covered sea ice

S. Willmes et al.

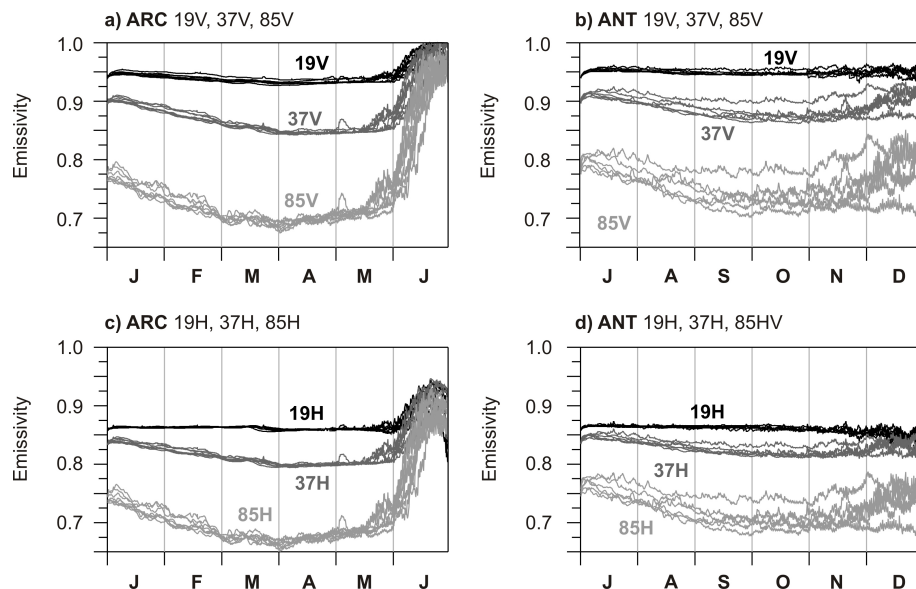


Fig. 3. The seasonal evolution of 19 GHz, 37 GHz and 85 GHz emissivities at vertical (**a** and **b**) and horizontal (**c** and **d**) polarizations for Arctic regions (**a** and **c**, January to June) and Antarctic regions (**b** and **d**, July to December). Data are averaged for the period from 2000–2009.

Title Page

Abstract

Introduction

Conclusions

References

Tables

Figures

◀

▶

◀

▶

Back

Close

Full Screen / Esc

Printer-friendly Version

Interactive Discussion



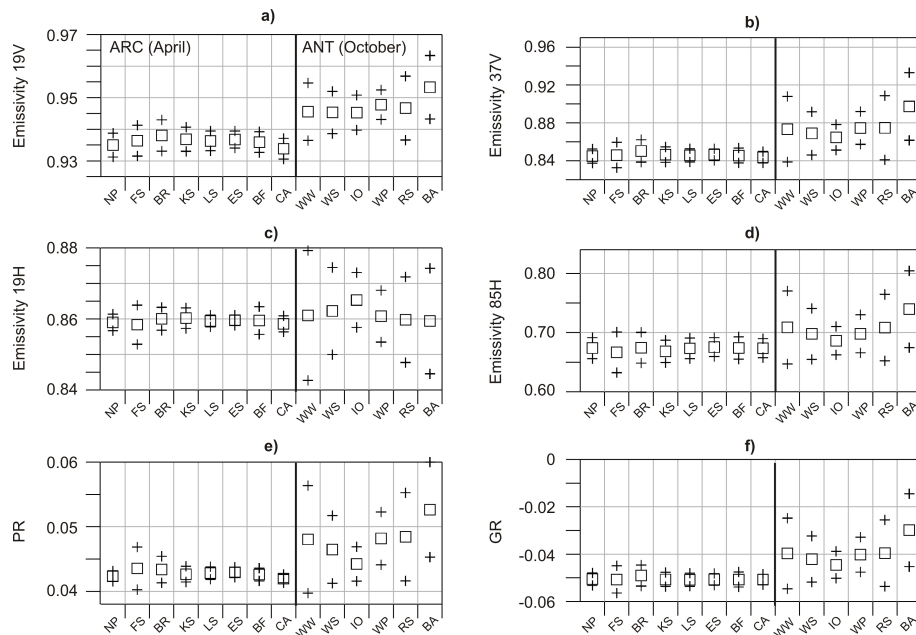


Fig. 4. Mean (squares) and standard deviation (crosses) of emissivity values indicating the daily, spatial and interannual variability of emissivity values in the 4th month of simulation (ARC: April, ANT: October) for emissivities at **(a)** 19V, **(b)** 37V, **(c)** 19H, **(d)** 85H as well as **(e)** Polarization Ratio and **(f)** Gradient Ratio.

Title Page

Abstract

Introduction

Conclusions

References

Tables

Figures

◀

▶

◀

▶

Back

Close

Full Screen / Esc

Printer-friendly Version

Interactive Discussion



Microwave emissivity variability of snow-covered sea ice

S. Willmes et al.

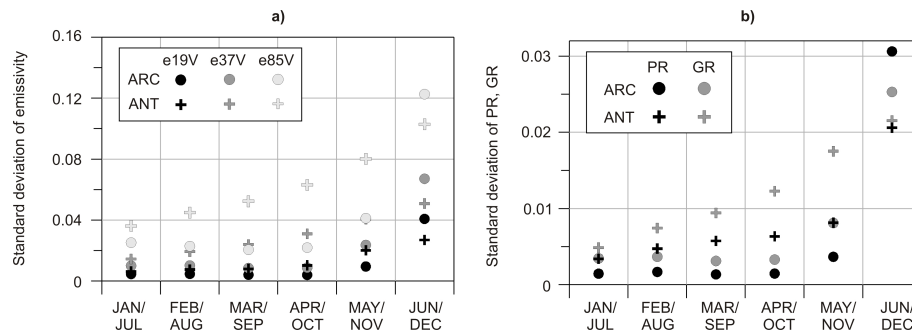


Fig. 5. Seasonal evolution of monthly standard deviations of **(a)** emissivities at 19 (black), 37 (gray) and 85 GHz (white), each at vertical polarization, for the Arctic (circles) and Antarctic (crosses), **(b)** PR (black symbols) and GR (grey symbols) for the Arctic (circles) and Antarctic (crosses). Monthly values, resuming the diurnal, regional and interannual variabilities, January to June (Arctic) and July to December, Antarctic, 2000–2009.

[Title Page](#)
[Abstract](#)
[Introduction](#)
[Conclusions](#)
[References](#)
[Tables](#)
[Figures](#)
[Back](#)
[Close](#)
[Full Screen / Esc](#)
[Printer-friendly Version](#)
[Interactive Discussion](#)

Microwave emissivity variability of snow-covered sea ice

S. Willmes et al.

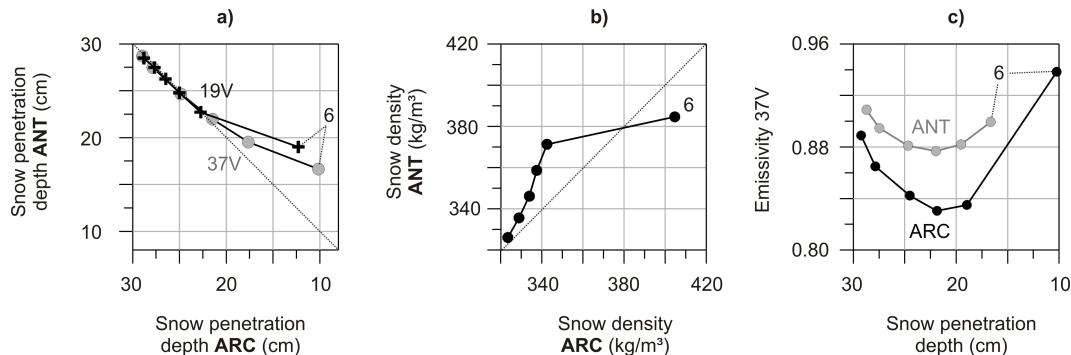


Fig. 6. (a) Monthly average snow penetration depth, Arctic vs. Antarctic for 19 V (black) and 37 V (grey), (b) Monthly average snow density, Arctic vs. Antarctic, (c) Monthly average 37 V emissivity in relation to snow penetration depth. Each for the months of January to June (Arctic) and July to December (Antarctic; last months are highlighted by number “6” to indicate the direction of the seasonal evolution), averaged for all regions, 2000–2009.